

Numerical Analysis of the Magnetohydrodynamic Flow and Heat Transfer in Microchannel

Mushtaq Ismael Hasan
Assist Prof. of Thi
Qare University
Iraq, Thi Qare Province,
University of Thi Qare

Abdul Jabbar F. Ali
Assist Prof. of
Wasit University
Iraq, Wasit Province,
University of Wasit

Rhan S. Tufah
University of Wasit
Iraq, Wasit Province,
University of Wasit

ABSTRACT

Magnetohydrodynamic micropumps received more attention due to its application in pumping of biological and chemical specimens, such as blood, DNA, and saline buffers. In this paper the MHD flow in square microchannel has been numerically investigate with different working fluids and electromagnetic boundary conditions, PBS solution and sea water have been used as working fluids. The study covers a selected range of applied electric currents and magnetic flux to explore their effects on MHD flow and heat transfer. Thermal characteristics of MHD flow have been also studied by calculation the temperature distribution through MHD micropump region. The results obtained show a considerable effect of both of the applied electric and magnetic fields on the velocity and flow rate. The sea water gave higher velocity and flow rate compared with PBS solution, and there is a slight increase in temperature due to small effect of Joule heating.

Nomenclature

B: Magnetic flux density vector (T), μ : Viscosity (Pa-s), ϕ : Electric potential (v), U: Flow velocity (m/s), E: Electric field (v), δ : Electric conductivity (s/m), F_L : Lorentz force (N), L_e : Electrode length (m), ρ : Fluid density (kg/m^3), C_p : Specific heat of fluid (J/Kg.k), K: Thermal conductivity (W/m.K).

Keywords

MHD flow; microchannel; micropump; numerical investigation; electromagnetic.

1. INTRODUCTION

Magnetohydrodynamic is the field of science that study the flow of the electrically conducting fluids subjected to electromagnetic forces. It is deals with the mutual interaction between electromagnetic fields and fluid flow. Non-magnetic and electrically conducting fluids must be used, which limits the application of hot ionized gases (plasmas), liquid metals and electrolytes [1]. In the last two decades application of microfluidic devices has rapidly extended to a wide variety of fields. Microfluidic devices are used in different applications such as reactors, micropumps, pressure flow sensors and mixers. The micropumps are the basic sign of the development of these devices. MHD micropump is one of the most important microfluidic systems that generates continuous flow without moving parts and is suitable for biomedical applications [2]. There are many investigations in the previous studies aimed to describe of the velocity profiles and other MHD parameters.

Lemoff and Lee (2000) [3] constructed a practical AC MHD pump in which the Lorentz force is used to propel an

electrolytic solution along a microchannel etched in silicon. Experimental measurements were conducted on various concentrations of sodium chloride (NaCl) solutions to determine the maximum current allowed in the microchannels before gas bubbles were observed. Their experimental results indicated that the electrolysis phenomenon was greatly reduced when the frequency of the applied current was sufficiently high. R. chaabane et al. (2007) [4] reported a numerical method based on the performance of MHD micro pump with Faraday electrode configuration evaluated by a 2D finite difference method. They concluded that the cited method achieved good convergence for pressure distribution and velocity field along the MHD duct. Their numerical simulations formulation shows that, the flow velocity of the electrolytic solution shows a maximum value along the axial direction of the MHD channel. Also the amplitudes of velocity and the pressure oscillation increased with the increasing of the current density and the magnetic flux density. M.H. Yazdi et al. (2011) [5] studied numerically the viscous dissipation term in energy equation and assumed the surface temperature to be linear. Also they solved the MHD flow and heat transfer of a regular fluid over a stretching sheet with the presence of chemical reaction. A. B. Ashikin and A. Rohana (2012) [6] investigated numerically the Viscous dissipation term in energy equation in MHD flow Also they investigated A stretching sheet with rising temperature of sheet that is linearly stretched. S. Mukhopadhyay (2013) [7] Studied numerically the MHD flow and heat transfer over an exponentially stretching permeable sheet. He investigated the flow and heat transfer characteristics in stretching sheet embedded in a thermally stratified medium. L. P. Aoki et al. (2013) [1] presented a closed water circuit with square channel filled with an electrolyte fluid. Their model was derived from the Navier-stokes equations for Newtonian fluid using the k- turbulence model and coupled with the Maxwell's equations. Their 3D numerical Simulations allowed obtaining realistic Predictions of Lorentz forces and current densities. Their results show that for the Lorentz force an M shape profile was observed, the velocity increased with increasing of the applied voltage and that the M shaped profile of the velocity is the consequence of the uneven distribution of Lorentz force and the condition of mass conservation. Kosuke Ito et al.(2014) [8] discussed the numerical and experimental researches on the fluid behavior in an MHD micro pump using a permanent magnet. They found that, the Hartmann flow is not observed in the channel due to very weak of MHD interaction, so that poiseuille flow is maintained in the channel. Their also examined numerically the influences of the channel height and the strength of applied magnetic flux density on the fluid temperature in the channel.

In this paper the MHD flow in microchannel will be studied numerically and the effects of electrical and magnetic parameters on MHD flow will be studied for two types of fluids.

2. PROBLEM DESCRIPTION

In the MHD micro pump, the pumping action is generated by the electromagnetic Lorentz Force generated from the applied magnetic field and electric current. The basic principle based on applying an electric current and orthogonal magnetic field across a channel filled with electrically conducting fluid [2], [9]. Fig.1 shows the description of the MHD pump studied where the electrical field is applied in the horizontal direction by two parallel electrodes and the magnetic field is applied in the vertical direction by two parallel magnets. As show Fig.1 the direction of flow is perpendicular on both of the electrical and magnetic fields created from the effect of Lorentz force generated by the interaction of electrical and magnetic fields. The formulation of MHD steady state model was derived from Maxwell equations coupled with Navier-stokes equations. Therefore the phenomena are described by the electro magnetism and the fluid dynamics equations [1], [10]. A phosphate buffered saline (PBS) solution and sea water are used as a working fluids. The thermo physical Properties of sea water and PBS solution are summarized in Table1 [4], [8].

Table 1 Physical properties of PBS & Sea water

Physical property	PBS	Sea water
Electrical conductivity [s/m]	1.59	4
Viscosity [Pa-s]	0.7×10^{-3}	1.9×10^{-3}
Mass density [kg/ms]	1020	1025
Specific heat [J/kg.K]	2920	4007

3. MATHEMATICAL MODEL

As illustrated in Fig.1 the studied MHD model consists of microchannel with square cross section with two parallel electrodes & two parallel magnets. The mathematical model for MHD flow can be divided into three sets of governing equations as below:

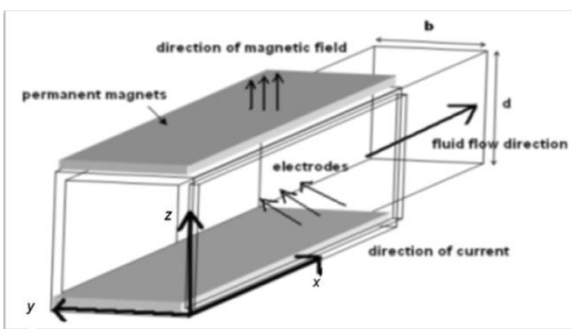


Fig.1 Schematic figure for the MHD micro pumps with a square cross section.

3.1. Electromagnetic System Of Equations

This system consists of the Maxwell Equations along with ohm's law. These equations describe the distribution of the magnetic flux density, the electric field and the current density. Magnetic induction equation shows that the motion of a conducting liquid in an applied magnetic field induces a

magnetic field in the medium through a $\nabla \times (u \times \beta)$ term. The induced magnetic field is neglected in this study due to the small values of magnetic Reynolds number Rem in typical electrolytes used in biological microfluidics applications [8], [11] and [12].

Maxwell Equations:

$$\nabla \cdot D = \rho \quad (1)$$

$$\nabla \cdot B = 0 \quad (2)$$

$$\nabla \times E = -\frac{\partial B}{\partial t} \quad (3)$$

$$\nabla \times H = J + \frac{\partial D}{\partial t} \quad (4)$$

By combining with Ohm's Law:

$$J = \delta(E + v \times B) \quad (5)$$

Steady Maxwell Equations:

$$\nabla \cdot J = 0 \quad (6)$$

$$\nabla \times E = 0 \quad (7)$$

Ohm's Low

$$J = \delta(E + u \times B) = \delta(-\nabla\phi + u \times B)$$

The Lorentz force is then given as:

$$F_L = (J \times B) \quad (8)$$

3.2. Fluid dynamic system of equations:

It consists of the continuity equation and momentum equation which define the physics of bulk fluid flow.

Continuity Equation:

$$\nabla \cdot U = 0 \quad (9)$$

Momentum equation:

$$\frac{du}{dt} + (u \cdot \nabla)u = -\frac{1}{\rho} \nabla P + \nu \nabla^2 + \frac{1}{\rho} (J \times B) \quad (10)$$

3.3. Thermal system of equations:

This system formed from the energy equation as follows:

$$\rho c \left(\frac{dT}{dt} + \mu \nabla T \right) = K \nabla^2 T + \frac{|J|^2}{\delta} \quad (11)$$

The dependency of electrical conductivity on fluid temperature is determined as follows [13]:

$$\delta = \delta_0 (1 + 0.02T) \quad (12)$$

The flow is assumed as an incompressible, steady and fully developed. The no slip assumption is made since velocities on walls in z and y directions are assumed to be zero. Also the surface tension is neglected. The 3D Magnetohydrodynamic equations presented above are solved with finite element method. An iterative solution approach was used [14], [15], the model is discretized with tetrahedral elements and a mesh with suitable size was selected. A mesh independence study has been done to explore the effect of mesh on the numerical solution and as can be seen from Table 2 that, after mesh 3 there is no considerable change in results, therefore and for more accuracy the third mesh has been used for all numerical calculations. The selected ranges for studied parameters are listed in table 3 for both PBS and sea water. And to close the numerical mode the boundary conditions used are summarized in Table 4. The governing equations were numerically solved and the distribution of velocity and temperature were calculated in the fluid through the channel.

Table 2 Mesh independence study

Mesh configuration	Flow rate [kg/s]	Maximum velocity [mm/s]
Mesh1 (No. of nodes = 382765)	3.1895e-7	4.12
Mesh2 (No. of nodes = 432531)	3.1892e-7	4.11
Mesh3 (No. of nodes = 497524)	3.1891e-7	4.11

Table 3 Ranges of studied parameters

Parameter	Range
Magnetic flux density B [T]	0.1 – 1
Applied DC current I [mA]	1 – 20
Channel height h [mm]	0.4
Electrode length [mm]	26
Initial temperature To [K]	300

Table 4 Boundary conditions

Equations set	Boundary condition
Electromagnetics	$B(x,y,0) = \text{constant} \quad (-13 \leq x \leq 13)$ $B(x,y,d) = \text{constant} \quad (-13 \leq x \leq 13)$ $\varphi(x,0,z) = V \quad (-13 \leq x \leq 13)$ $\varphi(x,b,z) = 0 \quad (-13 \leq x \leq 13)$ $\left(\frac{\partial \phi}{\partial n}\right)_{in} = \left(\frac{\partial \phi}{\partial n}\right)_{wall} = \left(\frac{\partial \phi}{\partial n}\right)_{out} = 0$ Electrically and Magnetically insulated elsewhere
Fluid dynamics	Inlet: $\frac{\partial u_{x,in}}{\partial x} = v = w = 0, p_{in} = 0$ Outlet: $P_{out} = 0$ Wall: $u = v = w = 0, \frac{\partial p_{wall}}{\partial n} = 0$
Thermal system	$T_{in} = T_o$ $T_{wall} = T_o$ $\frac{\partial T_{out}}{\partial x} = 0$

4. RESULTS AND DISCUSIONS

To check the validity of the present numerical model a validation has been made by solving the model presented in Kosuke I. et al. [8] and a comparison has been made between the results of present model and the experimental and numerical results of [8]. Fig.2 shows the distribution of

velocity with channel height as a comparison between present model with numerical and experimental data of Kosuke I. et al. [8]. From this figure it can be seen that, the agreement is very good between the results of present numerical model and numerical result of [8] and is accepted between present model and experimental data of [8]. The deviation between results of present model and experimental data of [8] may be due to difference in properties of fluids used. Same deviation can be observed between the numerical and experimental results of [8].

Fig. 3 represent a 2D velocity contour for PBS solution at $I = 10$ mA and $B = 0.5$ T at the midpoint of the MHD pump (center of electrodes and magnets region). This contour shows the distribution of velocity in y-z plan across the channel. It's clear from this figure that, the velocity distribution in z and y direction is the same due to uniform distribution of generated Lorentz force which lead to create the flow in the MHD pump region.

Fig.4 shows the variation of maximum velocity in the channel with applied electric current for magnetic flux of 0.5 T for both PBS solution and sea water. From this figure it can be seen that the velocity for both fluids increased with increasing the applied current at constant applied magnetic field, due to increasing of the Lorentz Force which cause extra flow in the MHD pump due to viscosity of fluids. Also it can be seen from this figure that, the velocity magnitude for sea water is larger than that for PBS solution for all selected range of applied current due to larger value of electrical conductivity for sea water, since the MHD micropump flow is highly depending on the electrical conductivity of the working fluid.

The variation of maximum velocity in the channel with applied magnetic field for electric current of 10 mA for both PBS and sea water is indicated in Fig.5. From this figure it can be noted that, the velocity for both fluids increased with increasing of the applied magnetic field at same value of applied current, due to increasing of the Lorentz Force as explained before. Also for all selected values of magnetic field the value of maximum velocity for sea water are higher than that for PBS as declared above.

Fig.6 represent the variation of flow rate in the channel with applied magnetic field for electric current of 10 mA for both PBS and sea water. From this figure it can be observed that, the flow rate for both fluids increased with increasing of the applied magnetic field at constant applied current, due to increasing of flow velocity as a result of increasing the Lorentz force.

Fig.7 shows the variation of flow rate in the channel with applied electric current for magnetic flux of 0.5 T for both PBS and sea water. From this figure one can observe that, the flow rate for both fluids increased with increasing the applied current, due to increasing the Lorentz Force as discussed before in fig.6. These two figures (5 and 6) show that, the performance of MHD micropump can be enhanced through increasing the flow rate produced by increasing the values of applied electric or magnetic fields even for fluids with low electrical conductivity.

Fig.8 shows the velocity distribution along channel height in the z-direction for PBS solution with electric current of 10 mA and different values of applied magnetic field. From this figure it can be seen that, the velocity is uniformly distributed across channel and it reach the parabolic shape due to uniform distribution of Lorentz force. It can be also seen that, the velocity is increased with increasing the applied magnetic

field at constant applied current, due to increasing the Lorentz Force.

The distribution of velocity along channel height in the z-direction for sea water with electric current of 10 mA and different values of applied magnetic field is shown in Fig.9. As explained in Fig.8 the velocity is uniformly distributed across channel and it reach the parabolic shape and it increased with increasing the applied magnetic field at constant applied current. Comparison between the results presented in figures (8 and 9) reveal that, the magnitudes of velocity for sea water are higher than that for PBS solution for all selected values of magnetic field due to higher electrical conductivity of sea water compared with PBS solution.

Fig.10 illustrate the tow-dimensional contour shows the distribution of temperature for PBS solution at $I = 10.0$ mA and $B = 0.5$ T. From this figure one can observe that, there is a slight increase in fluid temperature due to the effect of joule heating. And the temperature is uniformly distributed across the channel due to uniform distribution of joule heating.

Fig.11 depicts the temperature distribution along the channel width between two electrodes for sea water for selected values of electric current for applied magnetic field of 0.5 T. From this figure it can be noted that, the increasing in electric current concentrated at the edge of anode and cathode, where the electric current density is about twice as much as at the central point of the MHD micro pump. Since the Joule heating related to the square of electric current density, the Joule heating at the edge of electrodes is about four times more than that at the center of channel. The fluid temperature at the electrodes edge is much lower than that at the central point, and also it is almost equal to the wall temperature. Also it can be seen that, the temperature increased with the increasing of the electric current due to Joule heating effects

The temperature distribution along the channel width between two electrodes for PBS solution for a selected value of electric current for applied magnetic field of 0.5 T is shown in Fig.12. This figure indicate that, the distribution of temperature for sea PBS solution behave as in Fig. 11 for sea water as discussed there with higher values of temperature in case of PBS solution due to higher thermal properties of PBS solution compared with sea water.

Fig.13 shows the temperature distribution along channel height between two magnets for sea water for selected values of magnetic flux at applied current of 10 mA. From this figure it can be noted that, there is a rapid increase in temperature near the magnets and then the temperature remain constant along the remaining height due to concentration of joule heating near the magnets. Also it can be seen that, there is a slight increase in temperature with increasing magnetic flux due to increasing the Joule heating.

Fig.14 depicts the temperature distribution along channel height between two magnets for PBS solution for selected values of magnetic flux at applied current of 10 mA. From this figure it can be noted that, the trend of temperature in case of using PBS as working fluid is similar for sea water case except a slight increment in temperature with sea water compared with PBs due to higher value of the electrical conductivity for sea water compared with PBS.

5. CONCLUSIONS

Numerical analysis has been carried out to study the hydrodynamic and thermal characteristics of MHD micropump with deferent values of applied electric current and magnetic flux for two working fluids (Phosphate-

Buffered-saline solution and sea water). From the result obtained the following Conclusions can be drawn:

1. The created flow rate with its velocity MHD micropump are highly dependent on both of the magnetic and electrical fields, since by increasing of the magnetic flux density or the applied current, the velocity increased linearly as well as the flow rate.
2. Interaction of magnetic and electric fields in MHD micropump causes a slight increase in fluid temperature.
3. In a range of the flow rate (10-50) $\mu\text{l}/\text{min}$ required for biomedical analysis, the increasing in temperature with using of MHD micro pump is less than 1 K at an electric current up to 20 mA.
4. For a square cross suction channel the distribution of the velocity and temperature in z and y directions are the same.
5. The effect of electric current on the fluid temperature is higher than that for magnetic field.

Figure captions

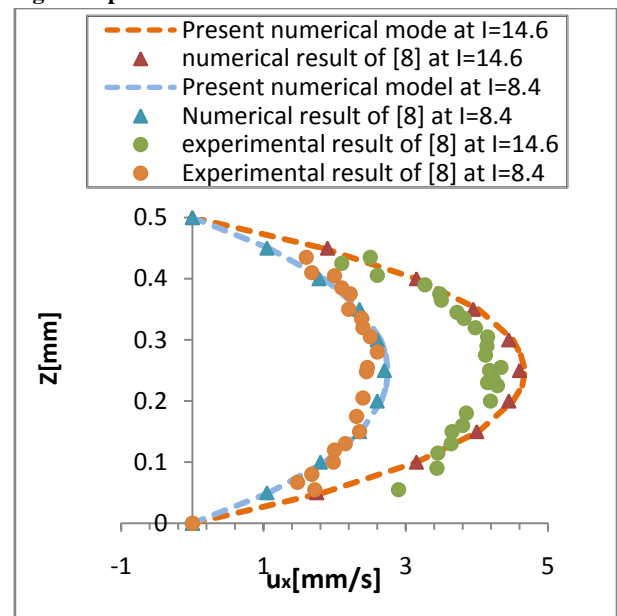


Fig.2 distribution of velocity as comparison between present numerical model and data of [8].

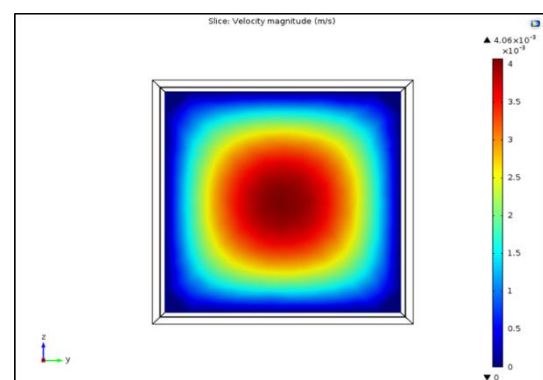


Fig.3 Velocity contour at the mid point of the electrode length

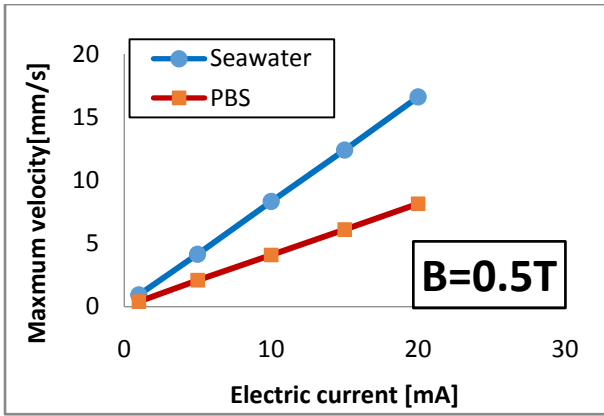


Fig.4 Variation of maximum velocity with applied current at constant magnetic flux.

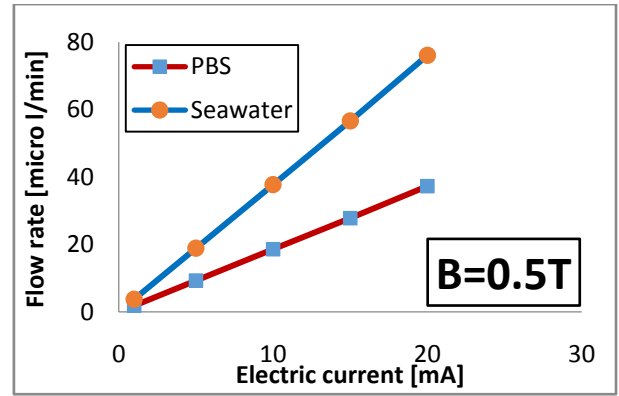


Figure 7. Variation of flow rate with applied electric current at constant magnetic flux.

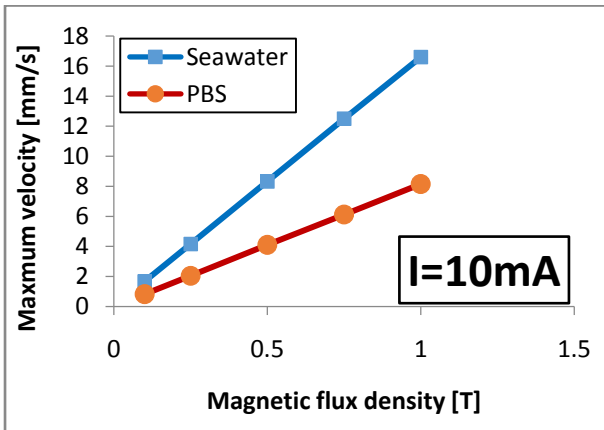


Fig. 5 Variation of maximum velocity with applied magnetic flux at constant electric current.

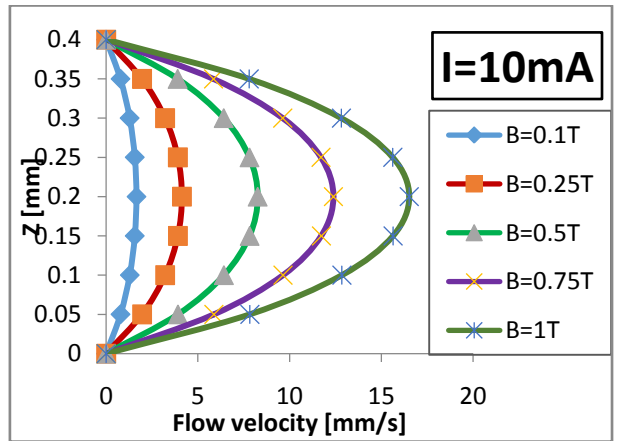


Fig.8 Velocity distribution along channel height for different magnetic flux densities for sea water.

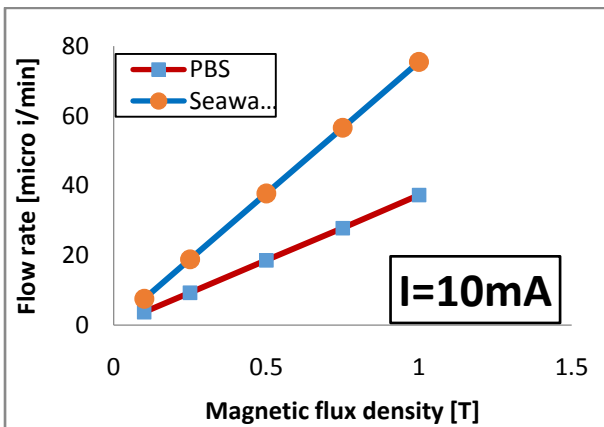


Fig.6 Variation of flow rate with applied magnetic flux density at constant current.

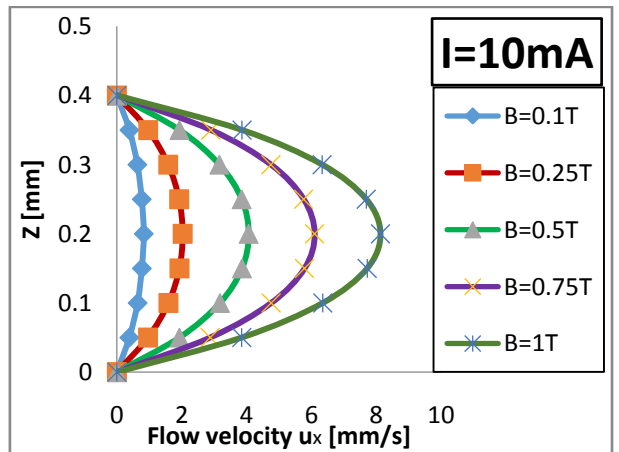


Fig.9 Velocity distribution along channel height for different magnetic flux densities for PBS solution.

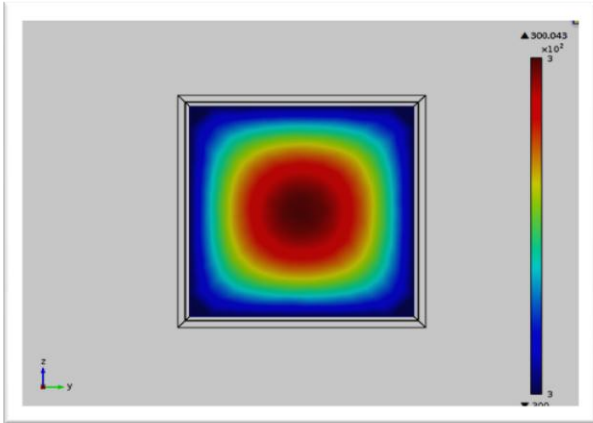


Fig.10 Temperature contour at cross sectional plan for PBS solution.

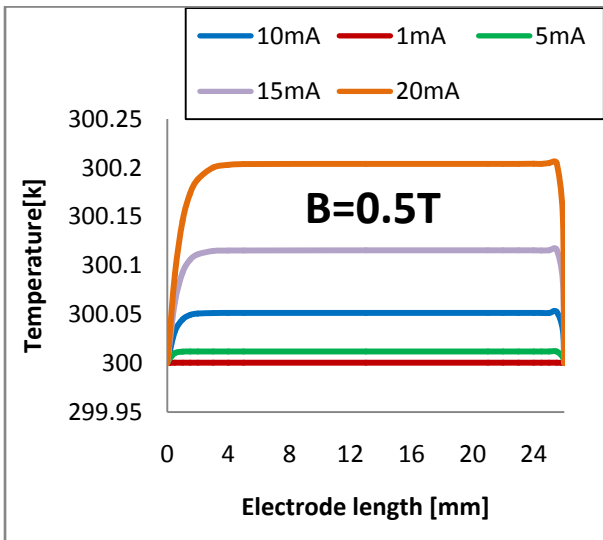


Fig.11 Distribution of temperature along the electrode for sea water at different applied current.

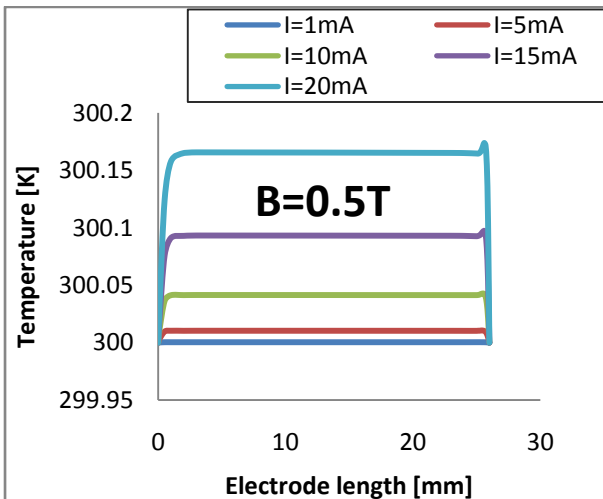


Fig.12 Distribution of temperature along the electrode for PBS solution at different applied current.

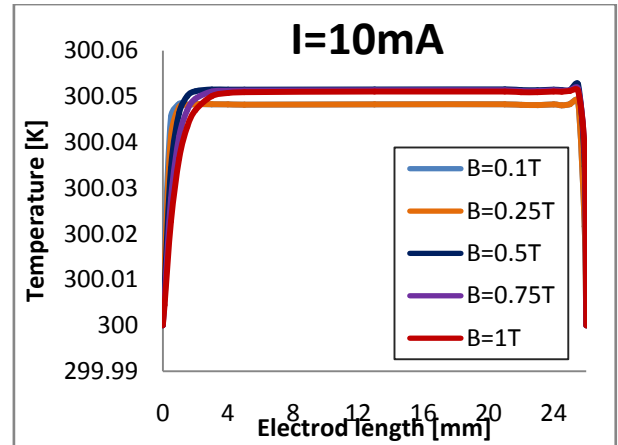


Fig.13 Temperature distribution along the electrode length for different values of magnetic flux for sea water.

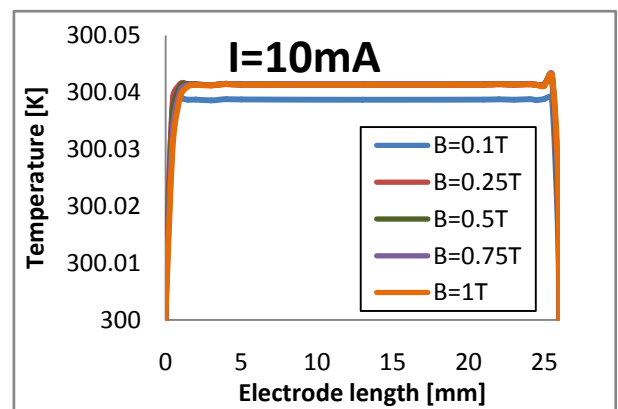


Fig.14 Temperature distribution along the electrode length for different values of magnetic flux density for PBS solution.

6. REFERENCES

- [1] Luciano P. A., Harry E. S., Michael G. M., "An MHD Study of the Behavior of an Electrolyte Solution using 3D Numerical Simulation and Experimental results", University of São Paulo, Comsol Conference in Boston ,2013.
- [2] Mehdi K., Nader P., Maqsood G., Iraj M., "Investigation Of Thermal Behavior And Fluid Motion In Direct Current Magneto hydrodynamic Pumps", Journal of Thermal Science, Vol. 18, pp. 551-562, 2014.
- [3] Lemoff, A, Lee, A., "An AC Magneto hydrodynamic Micropump", Sens. Actuators, Vol. 63, pp.178-185, 2000.
- [4] Raoudha C., Adam B., Sassi B. N., "Numerical Magneto Hydro Dynamic Flow Simulation of Velocity and Pressure for Electrically Conducting, Incompressible Fluids", Braz. Soc. of Mech. Sci. & Eng, Vol. XXIX, No. 3, pp. 299-306.
- [5] M.H. Yazdi, S. Abdullah and I. Hashim, "Slip MHD liquid flow and heat transfer over non-linear permeable stretching surface with chemical reaction, International", Journal of Heat and Mass Transfer, vol. 54, pp. 3214-3225, May 2011
- [6] A.B. Ashikin nad A. Rohana, "Boundary layer over a stretching sheet with a convective boundary condition

- and slip effect”, *World Applied Sciences Journal*. vol. 17, pp. 49-53, July 2012.
- [7] S. Mukhopadhyay, “MHD boundary layer flow and heat transfer over an exponentially stretching sheet embedded in a thermally stratified medium”, *Alexandria Engineering Journal*, vol. 5, no.8, pp. 12-19, 2013.
- [8] Kosuke I., Toru T., Takayasu F., Motoo I., " Influences of Channel Size and Operating Conditions on Fluid Behavior in a MHD Micro Pump for Micro Total Analysis System", *Journal of International Council on Electrical Engineering*, Vol. 4, No.3, pp.220-226, 2014.
- [9] Huang L., Wang W., Murphy M.C., Lian k., Ling Z.G., " LIGA fabrication and test of a dc type Magnetohydrodynamic (mhd) micropump", *Microsystem technologies*, vol. 6 ,pp.235-240,2000.
- [10] Farideh A., Haslina J. and Nurul A. M. Y., “A Comprehensive Study of Micropumps Technologies”, *Int. J. of Electrochemical Sciences*. Vol. 7, pp. 9765 – 9780, 2012.
- [11] Hughes W. F. and Young F. J." *The Electromagnetodynamics of Fluids*", John Wiley & Sons, New York, 1966.
- [12] Kateřina H., Karel F., "CFD SOLUTION of MHD", *Journal of applied science in the thermodynamics and fluid mechanics*, Vol. 5, No. 2, 2011.
- [13] Vaibhav,D. Patel and Samuel. K. Kassegne,"Electroosmosis and thermal effects in magnetohydrodynamic (MHD) micropumps using 3D MHD equations", *Sensors and Actuators B, Chemical* 122, pp. 42-52, 2007.
- [14] Mian Q. and Haim H. B., “Magneto-Hydrodynamic Flow in Electrolyte Solutions”, *COMSOL Conference Boston*, pp.1-7, 2009.
- [15] Aoki L. P., Maunsell M. G, and Schulz H. E., “A MAGNETOHYDRODYNAMIC STUDY OF BEHAVIOR IN AN ELECTROLYTE FLUID USING NUMERICAL AND EXPERIMENTAL SOLUTIONS”, *Engenharia Térmica (Thermal Engineering)*, Vol. 11, No. 1-2, pp. 53-60, 2012.